Modeling of HTPEM Fuel Cell Start-Up Process by Using Comsol Multiphysics

Y. Wang[*1,2], J. Kowal[1,2] and D. U. Sauer[1,2,3]
[1] Electrochemical Energy Conversion and Storage Systems Group, Institute for Power Electronics and Electrical Drives (ISEA), RWTH Aachen University, Germany
[2] Juelich Aachen Research Alliance, JARA-Energy, Germany
[3] Institute for Power Generation and Storage Systems (PGS), E.ON ERC, RWTH Aachen University, Germany
*Jaegerstrasse 17/19, D-52066 Aachen, Germany, email: batteries@isea.rwth-aachen.de

Abstract: High temperature PEM fuel cells are considered to be the next generation fuel cells. The electrochemical kinetics for electrode reactions are enhanced by using PBI membrane at an operation temperature between 160 °C and 180 °C comparing to low temperature PEM fuel cells. But starting HTPEM fuel cells from room temperature to a proper operation temperature is a challenge. There are different methods to start HTPEM fuel cells. In this work, using preheated air to heat up the fuel cells through the gas channels or cooling channels and their combinations with ohmic heating by fuel cell reaction are investigated. Based on a 3D Comsol model of a single HTPEM fuel cell, start-up process is analyzed by comparing start-up time and thermal behaviors inside the fuel cell. Finally, optimal start-up methods are proposed for the HTPEM fuel cell.

Keywords: HTPEM fuel cell, 3D Comsol model, start-up process, thermal behavior

1. Introduction

High temperature PEM (proton exchange membrane/polymer electrolyte membrane) fuel cells are considered the next generation fuel cells. The electrochemical kinetics for electrode reactions are enhanced by using PBI (Polybenzimidazole) membrane at an operation temperature between 160 °C and 180 °C comparing to low temperature PEM fuel cells. Besides this by using PBI membrane, gases do not need to be humidified and the water produced by the reaction has only one phase. Therefore water management is unnecessary. This simplifies the HTPEM fuel cell system. In addition, higher CO tolerance makes it possible to simplify the fuel processing system by integrating the fuel cell with a fuel processing unit (e.g. reformer).

For HTPEM, the fuel cell's temperature is a critical parameter. Zhang [1] investigated the dependency of cell performance on temperature. In the range of 120-180 °C, by increasing the temperature the cell power density increases and the membrane resistance decreases. Parrondo [2] got similar results and concluded that 180 °C is the optimal operation for HTPEM fuel cells. But for long-term operation, Oono [3] had a different conclusion. After fuel cell durability test at three different temperatures 150 °C, 170 °C and 190 °C, it was clarified that a higher cell temperature results in a higher cell voltage, but a shorter cell life. In order to keep the HT PEM fuel cells in a proper operation temperature during operation, Reddy [4] developed thermal management strategies for electrical vehicle application. Because of the higher operation temperature, starting HTPEM fuel cells from room temperature to operation temperature is also a challenge. In the work of Andreasen [5], the fuel cell stack is heated by using heating cartridges assembled in end plate or heating mats assembled on the edge of the stack. Singdeo [6] summarized different heat strategies for HTPEM fuel cells including direct electrical heating, reactant heating, coolant heating and ohmic heating. With the help of Comsol, Siegel [7-10] and Ubong [11] simulated mass transport, temperature distribution and etc. in HTPEM fuel cells based on 2D and 3D models. In Siegel's work [12], temperature distributions in gas channels are measured for different gas channel designs under both of no load and load operating conditions.

In practice, direct electrical heating not only needs extra heating materials but also can't heat up HTPEM fuel cell to a proper temperature symmetrically. Because of the thermal losses to environment, the temperature on the cell edge is still too low, when the temperature in central areas of the cell reaches the desired temperature.

So the direct electrical heating is not considered in this work. In this study, preheated air is used to heat up the fuel cells either through the gas channels or through cooling channels. Start-up time is compared for different air flow rates. Secondly, after the fuel cell temperature reaches 120 °C, fuel cell reaction can be started which speeds up the cell start-up process. The combined start-up processes of preheated air heating and ohmic heating by fuel cell reaction are investigated. The start-up time and cell temperature distribution are studied accordingly. Finally, based on the 3D Comsol model optimal start-up methods are proposed for the HTPEM fuel cell.

2. Model Geometry

To simplify the model and save simulation time, the outer dimension of the single HTPEM fuel cell has the same value with active area 90 mm x 50 mm. Figure 1 a) shows the single cell structure with different components. In the middle is the PBI including GDL, catalyst and membrane. On both sides of the PBI are the serpentine anode and cathode gas channel, which consists of six parallel channels of dimension 1.2 mm x 1.2 mm each. The straight parallel channels outside of the gas channels are cooling channels of dimension 1.5 mm x 2 mm, 20 channels on each side. These gas and cooling channels are separated by bipolar plates. On the outside of the cooling channels are two other bipolar plates, they can be assembled either with current collector and endplate to be a single cell or with other cells to be a stack. The integrated single cell is shown in Figure 1 b).

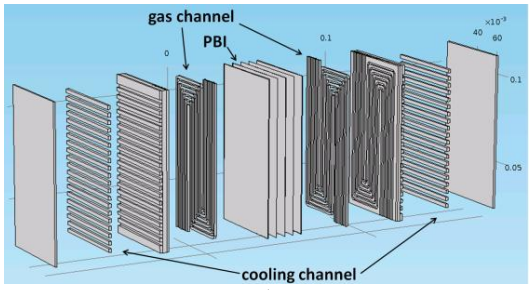

a)

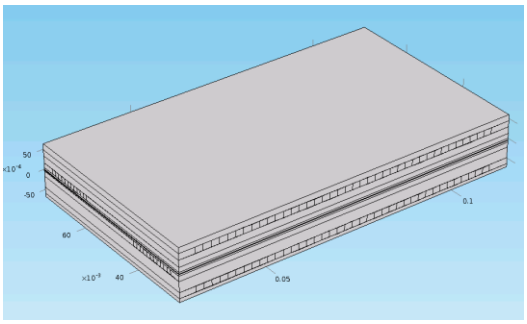
b)

Figure 1. HTPEM fuel cell structure a) single cell with different components, b) integrated single cell

3. Assumptions

In this model, the following assumptions are used [7-8]:

1) all gases and water are in gaseous phase
2) reaction gases are treated as ideal gas
3) laminar flow in all channels
4) all material parameters are constant
5) no crossover of gases and water through the membrane

4. Governing Equations

The HTPEM fuel cell is described in the Comsol model by different physics for momentum transfer, mass transfer, charge balances, electrochemical current and heat transfer.

4.1 Free and Porous Media Flow

Navier-Stokes for compressible flow (Ma<0.3) describes the gas flow / momentum transfer through the anode and cathode gas channels

$$\nabla \cdot (\rho \boldsymbol{u}) = 0 \tag{1}$$

$$\rho(\boldsymbol{u} \cdot \nabla)\boldsymbol{u} = \nabla \cdot \left[-p\boldsymbol{I} + \mu(\nabla \boldsymbol{u} + (\nabla \boldsymbol{u})^T) - \frac{2}{3}\mu[\nabla \cdot \boldsymbol{u}]\boldsymbol{I}\right] + \boldsymbol{F}$$

and through the porous media including GDL and catalyst layer.

(2)

$$\nabla \cdot (\rho \boldsymbol{u}) = Q_{br}$$
$$\frac{\rho}{\varepsilon_p}\left((\boldsymbol{u}\cdot\nabla)\frac{\boldsymbol{u}}{\varepsilon_p}\right) =$$
$$\nabla\cdot\left[-p\boldsymbol{I} + \frac{\mu}{\varepsilon_p}(\nabla\boldsymbol{u} + (\nabla\boldsymbol{u})^T) - \frac{2\mu}{3\varepsilon_p}(\nabla\cdot\boldsymbol{u})\boldsymbol{I}\right]$$
$$-\left(\frac{\mu}{k_{br}} + \beta_F|\boldsymbol{u}| + Q_{br}\right)\boldsymbol{u} + \boldsymbol{F}$$

In (1), ρ is gas mixture density [kg·m^{-3}], $\boldsymbol{u}$ gas mixture velocity vector [m·s^{-1}], p pressure [Pa], $\boldsymbol{I}$ identity matrix [-], μ dynamic viscosity [Pa·s], $\boldsymbol{F}$ body force vector [N·m^3]. In (2), Q_{br} is mass source or mass sink source term [kg·m^{-3}·s^{-1}], ε_p porosity of porous media [-], k_{br} permeability of porous media [m^2].

4.2 Transport of Concentrated Species

In this physics interface, Maxwell-Stefan multicomponent diffusion solves the mass transfer with following equation.

(3)

$$\frac{\partial}{\partial t}\rho\omega_i + \nabla\cdot\left\{-\rho\omega_i\sum_k D_{ik}\left[\nabla x_k + (x_k-\omega_k)\frac{\nabla p_A}{p_A}\right] - D_i^T\frac{\nabla T}{T}\right\} + \rho(\boldsymbol{u}\cdot\nabla)\omega_i = R_i$$

Here subscript i,k is for different species in gas mixture, ω_i, ω_k mass fraction [-], D_{ik} multicomponent Fick diffusivities [m^2·s^{-1}], x_k mole fraction [-], p_A pressure [Pa], D_i^T thermal diffusion coefficient [kg·m^{-1}·s^{-1}], T temperature [K]. R_i is source term caused by chemical reactions [kg·m^{-3}·s^{-1}]. The reaction rates for PEM fuel cell are described by following equations.

(4)

$$R_{H_2} = -\frac{i_a}{2F}M_{H_2}$$

$$R_{O_2} = -\frac{|i_c|}{4F}M_{O_2}$$

$$R_{H_2O} = \frac{|i_c|}{2F}M_{H_2O}$$

Here i_a / i_c is current density at anode / cathode catalyst layer [A·m^{-2}], they are calculated by equations (7) and (8). F is Faraday constant [C·mol^{-1}], M_{H2} / M_{O2} / M_{H2O} molecular mass [kg·mol^{-1}].

4.3 Secondary Current Distribution

The following general equations describe the potential distributions in electrolyte or electrode.

(5)

$$\nabla\cdot i_k = Q_k$$
$$i_k = -\sigma_k\nabla\phi_k$$

The equation (6) describes the charge balance in porous electrode. The charge transfer reaction calculated with (7) and (8) is a source or a sink in the porous electrode.

(6)

$$\nabla\cdot i_k = A_V\cdot i_{loc}$$

k denotes an index that is l for the electrolyte or s for the electrode. i_k is current density [A·m^{-2}]. Q_k is a general source term, which is i_a / i_c for electrolyte and -i_a / -i_c for electrode. σ_k is conductivity [S·m^{-1}], ϕ_k potential [V], A_v specific surface area of the electrocatalyst. i_{loc} is local charge transfer current density [A·m^{-2}], which is i_a / i_c on anode / cathode calculated by equation (7) / (8).

The linearized Butler-Volmer equation (7) can be used for small overpotential, which is suitable for anode of PEM fuel cell. And for cathode of PEM fuel cell, cathodic Tafel equation (8) is used. The overpotential can be also described by (9).

(7)

$$i_a = \left(\frac{(\alpha_a+\alpha_c)Fi_0}{RT}\right)\eta$$

(8)

$$i_c = -i_0\cdot 10^{\eta/A_a}$$

(9)

$$\eta_m = \phi_s - \phi_l - E_{eq,m}$$

In equations (7) and (8), i_0 is the exchange current density [A·m^{-2}], α_a anodic charge transfer coefficient, α_c cathodic charge transfer coefficient, R gas constant [J·mol^{-1}·K^{-1}], η overpotential [V], A_a Tafel slope. In (9), index m denotes both electrode reactions, on anode or cathode side. $E_{eq,m}$ denotes the equilibrium potential for reaction m.

4.4 Heat Transfer

Heat transfer is calculated by the two equations below in solid (10) and in fluid (11).

$$\rho C_p \frac{\partial T}{\partial t} - \nabla \cdot (k\nabla T) = Q \quad (10)$$

$$\rho C_p \frac{\partial T}{\partial t} + \rho C_p \boldsymbol{u} \cdot \nabla T = \nabla \cdot (k\nabla T) + Q \quad (11)$$

C_p is heat capacity [J·kg^{-1}·K^{-1}], k thermal conductivity [W·m^{-1}·K^{-1}]. Q is heat source or sink [W·m^{-3}], which includes irreversible joule heating due to charge transport in electrode and electrolyte, irreversible reaction heating due to overpotential and reversible heating due to entropy changes.

5. Boundary Conditions

The boundary conditions for the model in this study are as follows:

1) continuity at all internal boundaries
2) no slip boundary condition for all channel walls
3) all initial values set to zero
4) velocity and temperature defined at channel inlet, step function used for these two parameters in time dependent study
5) no backpressure at channel outlet, convective flux boundary conditions applied
6) constrain outer edges set to zero for both inlet and outlet
7) bipolar plates on the most side of the cell set to electric ground and cell operation potential
8) HTPEM fuel cell is insulated from environment

6. Simulation Results

In this section, start-up process is simulated with cooling channel or gas channel heating firstly. And then ohmic heating starts, when the membrane average temperature reaches 120 °C. Since HTPEM fuel cell can't work at a temperature lower than 120 °C. At a lower temperature, part of reaction produced water is still liquid form, which will damage the PBI membrane. The combinations of cooling/gas channel and ohmic heating are simulated secondly.

6.1 Start-up by cooling or gas channel heating

Figure 2 and 3 show the average membrane temperature changes according to different cooling/gas channel flow rates: 0.001 m/s, 0.01 m/s, 0.1 m/s and 1 m/s. The initial cell temperature is 20 °C and the input air of cooling/gas channel has a temperature of 160 °C. The start-up time of average membrane temperature reaching 120 °C is recorded in Figure 4 for different flow rates. It illustrates that start-up process by cooling channel heating is much faster than gas channel heating with same flow rate, about 25% of gas channel heating time. Flow rate influences start-up time of gas channel heating more than cooling channel heating. Start-up time does not decrease by increasing the cooling channel flow rate from 0.001 m/s to 1 m/s, but it decreases around 17% when the gas channel flow rate increases from 0.001 m/s to 1 m/s.

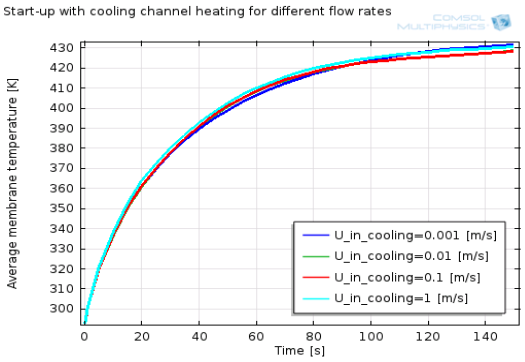

Figure 2. Start-up with cooling channel heating for different flow rates

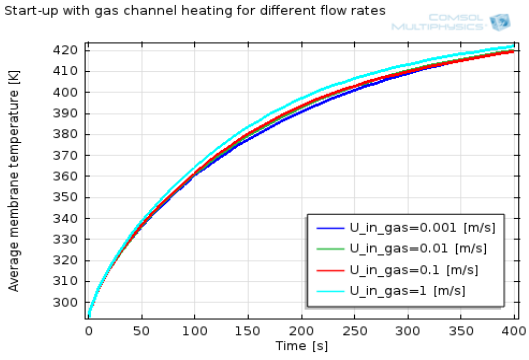

Figure 3. Start-up with gas channel heating for different flow rates

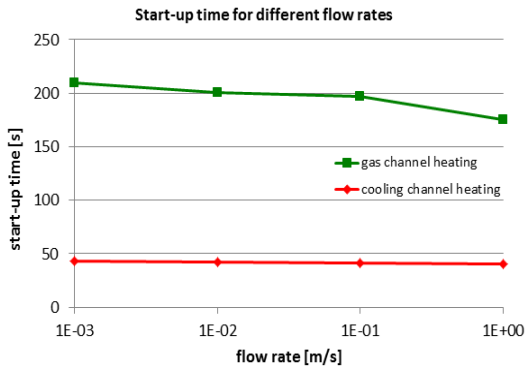

Figure 4. Start-up time comparison for different flow rates (average membrane temperature: 120 °C)

6.2 Start-up by ohmic heating with/without cooling channel heating

With the heating methods introduced in the last section, the fuel cell can be heated up from room temperature. When the membrane average temperature reaches 120 °C, to start the reaction can speed up the heating process. After 40 s heating by cooling channel, the average membrane temperature reaches 120 °C, and Figure 5 shows the start-up process with ohmic heating (cell voltage: 0.7 V) and cooling channel heating. Figure 6 shows the temperature's increase by ohmic heating after 180 °C gas channel heating. Both of the cooling channel and gas channel have a flow rate of 0.5 m/s.

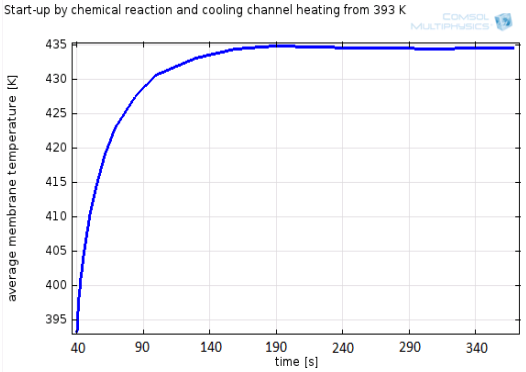

Figure 5. Start-up with chemical reaction and cooling channel heating from 120 °C/393 K (gas and cooling channel flow rate: 0.5 m/s)

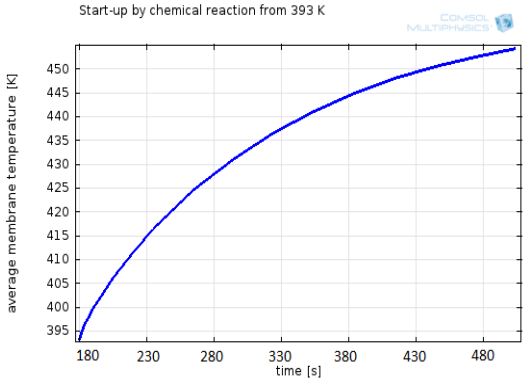

Figure 6. Start-up with chemical reaction from 120 °C/393 K (gas channel flow rate: 0.5 m/s)

The start-up of four different methods is shown in Figure 7 with a cooling/gas channel flow rate 0.5 m/s. The blue/violet line shows the start-up time only by cooling/gas channel heating. Ohmic heating (in red and green) starts after 40 s cooling channel heating and 180 s gas channel heating respectively. Cooling channel heating in blue is much faster than gas channel heating in violet which is already discussed in last section. Comparing the red and green curves, the combination of ohmic and cooling channel heating is better than only with ohmic heating, since cooling channel transfers extra heat to fuel cell. What should also be mentioned is, in the red line membrane temperature stops to increase when it reaches 160 °C /433 K. This is because of the cooling effect of air (160 °C) through the cooling channels. On the contrary, reaction (green line) heats up the fuel cell continuously, even when the membrane temperature reaches 160 °C/433 K.

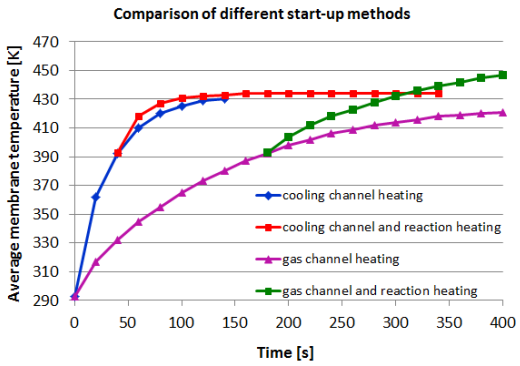

Figure 7. Start-up with different heating methods (gas and cooling channel flow rate: 0.5 m/s)

Figure 8 and 9 are the membrane temperature changes according to the start-up time by different start-up methods. In Figure 8, a) and b) show the membrane temperature distribution after 10 s by cooling channel and gas channel heating. The cooling channel inlets are on the bottom and gas channel inlets are on the right side of the membrane. The temperature in a) is already higher than in b) just after 10 s heating. In figure c) after 50 s cooling channel heating, the minimal membrane temperature reaches 388 K. But for gas channel heating in d) it takes 220 s to get this temperature. The last two figures e) and f) show the membrane temperature only by cooling channel heating at 140 s and gas channel heating at 280 s.

After 40 s cooling channel heating or 180 s gas channel heating, the average membrane temperature gets to 120 °C, fuel cell chemical reaction starts. a) and b) in Figure 9 show the temperature distribution at 50 s (after 10 s ohmic heating together with cooling channel heating) and 220 s (after 40 s ohmic heating without cooling channel heating). Comparing these figures with c) and d) in Figure 8, the temperature increases obviously after fuel cell reaction starts. Similar phenomenon can be observed in c) and d) in Figure 9 and e) and f) in Figure 8. To compare c) and d) in Figure 9 with each other, the temperature after 100 s ohmic heating (at 140 s) together with cooling channel heating is higher than after 100 s ohmic heating (at 280 s) only by chemical reaction. This result is in good agreement with Figure 7. To continue the simulation, membrane temperature keeps at around 433 K in e) in Figure 9 because of the cooling channel flow at 160 °C/433 K. But in f), it reaches the temperature limit 180 °C/453 K for PBI membrane at 415 s. At a higher temperature, effusion of phosphoric acid in PBI occurs. In f), temperature on the right edge is lower than other areas. That is because the air flow in gas channel (160 °C) works also as coolant, when the cell temperature exceeds 160 °C.

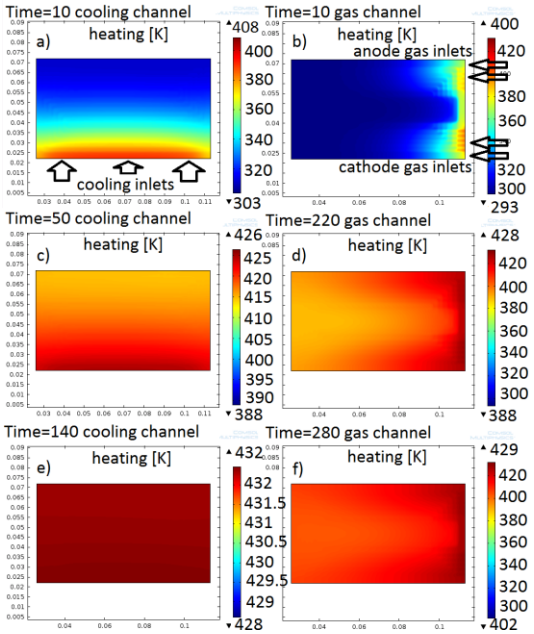

Figure 8. Membrane temperature distribution with cooling channel heating (left), with gas channel heating at (right)

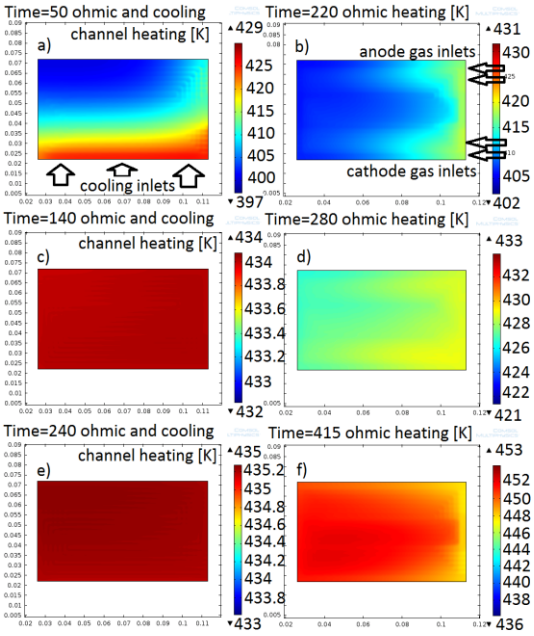

Figure 9. Membrane temperature distribution with reaction and cooling channel heating (left), only with reaction heating (right)

7. Conclusions

In this work, different start-up methods are simulated and analyzed based on Comsol Multiphysics. These methods include preheated air through cooling channel or gas channel and their combinations with ohmic heating (chemical reaction). Start-up by cooling channel heating is much faster than gas channel heating with same flow rate. Flow rate influences start-up time of gas channel heating more than cooling channel heating. Ohmic heating started from 120°C cell temperature speeds up heating process. Its combination with cooling channel heating can stabilize the cell temperature at coolant temperature. To sum up, the combination of ohmic and cooling channel heating is the optimal start-up process for this cell configuration.

8. References

1. J. Zhang, Y. Tang, C. Song, J. Zhang, Polybenzimidazole-Membrane-Based PEM Fuel Cell in the Temperature Range of 120-200 °C, *Journal of Power Sources*, **172**, 163-171 (2007)
2. J. Parrondo, C. V. Rao, S. L. Ghatty, B. Rambabu, Electrochemical Performance Measurements of PBI-Based High-Temperature PEMFCs, International *Journal of Electrochemistry*, **2011**, Article ID 261065, 8 pages (2011)
3. Y. Oono, T. Fukuda, A. Sounai, M. Hori, Influence of Operating Temperature on Cell Performance and Endurance of High Temperature Proton Exchange Membrane Fuel Cells, *Journal of Power Sources*, **195**, 1007-1014 (2010)
4. E. H. Reddy, S. Jayanti, Thermal Management Strategies for A 1 kWe Stack of a High Temperature Proton Exchange Membrane Fuel Cell, *Applied Thermal Engineering*, j.applthermaleng.2012.04.041 (2012)
5. S. J. Andreasen, S. K. Kar, Modelling and Evaluation of Heating Strategies for High Temperature Polymer Electrolyte Membrane Fuel Cell Stacks, *International Journal of Hydrogen Energy*, **33**, 4655-4664 (2008)
6. D. Singdeo, T. Dey, P. C. Ghosh, Modelling of Start-Up for High Temperature Polymer Electrolyte Fuel Cells, *Energy*, **36**, 6081-6089 (2011)
7. C. Siegel, G. Bandlamudi, A. Heinzel, Numerical Simulation of a High-Temperature PEM (HTPEM) Fuel Cell, Published in: Proceedings of the COMSOL Conference, Grenoble, France (2007)
8. C. Siegel, G. Gandlamudi, A. Heinzel, Modeling Polybenzimidazole/Phosphoric Acid Membrane Behaviour in a HTPEM Fuel Cell, Published in: Proceedings of the COMSOL Conference, Hannover, Germany (2008)
9. C. Siegel, G. Bandlamudi, N. van der Schoot, A. Heinzel, Large Scale 3D Flow Distribution Analysis in HTPEM Fuel Cells, Published in: Proceedings of the COMSOL Conference, Milan, Italy (2009)
10. C. Siegel, G. Bandlamudi, P. Beckhaus, A. Heinzel, Approaches for Fuel Cell Stack Modeling and Simulation with COMSOL Multiphysics, Published in: Proceedings of the COMSOL Conference, Paris, France (2010)
11. E. U. Ubong, Z. Shi, X. Wang, Three-Dimensional Modeling and Experimental Study of a High Temperature PBI-Based PEM Fuel Cell, *Journal of The Electrochemical Society*, **156 (10)**, B1276-B1282 (2009)
12. C. Siegel, G. Bandlamudi, A. Heinzel, Solid-Phase Temperature Measurements in a HTPEM Fuel Cell, *International Journal of Hydrogen Energy*, **36**, 12977-12990 (2011)

9. Acknowledgements

This work has been done in the framework of the research initiative “Tubitak” funded by the German Federal Ministry for Education and Research. Responsibility for the content of this publication lies with the author.